A harmonic transition state theory model for defect initiation in crystals

2013 Modelling Simul. Mater. Sci. Eng. 21 025010

(http://iopscience.iop.org/0965-0393/21/2/025010)

Modelling Simul. Mater. Sci. Eng. **21** (2013) 025010 (15pp) doi:10.1088/0965-0393/21/2/025010

A harmonic transition state theory model for defect initiation in crystals

T J Delph[1,4], P Cao[2], H S Park[2] and J A Zimmerman[3]

[1] Department of Mechanical Engineering and Mechanics, Lehigh University, Bethlehem, PA 18015, USA
[2] Department of Mechanical Engineering, Boston University, Boston, MA 02215, USA
[3] Mechanics of Materials Department, Sandia National Laboratories, Livermore, CA 94550, USA

E-mail: tjd1@lehigh.edu

Received 10 April 2012, in final form 6 November 2012
Published 1 February 2013
Online at stacks.iop.org/MSMSE/21/025010

Abstract

We outline here a model for the initiation of defects in crystals based upon harmonic transition state theory (hTST). This model combines a previously developed model for zero-temperature defect initiation with a multi-dimensional hTST model that is capable of accurately predicting the effects of temperature and loading rate upon defect initiation. The model has several features that set it apart from previous efforts along these lines, most notably a straightforward method of determining the energy barrier between adjacent equilibrium states that does not depend upon *a priori* information concerning the nature of the defect. We apply the model to two examples, triaxial stretching of a perfect fcc crystal and nanoindentation of a gold substrate. Very good agreement is found between the predictions of the model and independent molecular dynamics (MD) simulations. Among other things, the model predicts a strong dependence of the defect initiation behavior upon the loading parameter. A very attractive feature of this model is that it is valid for arbitrarily slow loading rates, in particular loading rates achievable in the laboratory, and suffers from none of the limitations in this regard inherent in MD simulations.

(Some figures may appear in colour only in the online journal)

1. Introduction

Transition state theory (TST) was originally developed in the field of chemical reaction kinetics, e.g. Henriksen and Hansen (2008), as a tool to describe the time-dependent process by which atoms or molecules leave one equilibrium state and transition to another state, the two states being separated by an intervening energy barrier on a potential energy surface of fairly high dimension. The process by which atoms break and reform chemical bonds has a good deal in

[4] Author to whom any correspondence should be addressed.

common with the process by which defects are initiated in solids. Accordingly there has been recent interest in using TST to model various defect formation phenomena in crystals, e.g. Mason *et al* (2006), Zhu *et al* (2008), Hara and Li (2010), Jin *et al* (2010), Ryu *et al* (2011), Nguyen *et al* (2011) and Weinberger *et al* (2012). TST has a number of attractive features in this regard, among them the ability to predict the temperature and time dependence of defect nucleation. Moreover it is valid for arbitrarily slow loading or deformation rates, much lower than those for which molecular dynamics (MD) simulations are typically feasible.

Key to the development of any TST model is a description of the TST rate factor k, also known as the nucleation rate. The rate factor includes both a prefactor and an exponential term involving the energy barrier to defect nucleation. In harmonic transition state theory (hTST), the prefactor depends upon the curvatures of the potential energy surface at a given equilibrium position. To date, applications of hTST to the problem of defect nucleation have made use of one-dimensional models that involve only a single component of curvature to calculate the prefactor. Various techniques have been used to estimate the energy barrier. Mason *et al* (2006) assumed the energy barrier to be linearly dependent upon the product of a scalar stress measure with an activation volume, this latter quantity being determined from a fit to experimental data. Later authors (Zhu *et al* 2008, Hara and Li 2010, Jin *et al* 2010, Ryu *et al* 2011, Nguyen *et al* 2011 and Weinberger *et al* 2012) have used a considerably more sophisticated numerical technique, the nudged elastic band method (Henkelman *et al* 2000, Zhu *et al* 2007), to determine the lowest saddle point adjacent to the equilibrium position on the potential energy surface.

In the present paper, we describe an hTST model that combines hTST with a recently developed model, called the Wallace criterion for brevity, for zero-temperature defect nucleation (Delph *et al* 2009, Delph and Zimmerman 2010, Yun *et al* 2011). The resulting formulation differs in several significant respects from previous work. In particular, the energy barrier appearing in the TST rate factor, a crucial component of the model, is determined in a rather direct fashion by finding the nearest saddle point along the loading path on the potential energy surface. The model also uses a relatively large number of curvature components on the potential energy surface to calculate the prefactor for the hTST rate factor. As judged by comparisons to MD simulations, the resulting model is capable of making accurate predictions of the loading rate and temperature dependence of defect nucleation in crystals. However, in contrast to MD techniques, the model is applicable for arbitrary slow loading rates and times, in particular for those achievable in the laboratory.

2. The hTST model

In the TST scenario, thermal excitation causes groups of atoms to travel from an equilibrium position on the potential energy surface for a deformed crystal to an adjacent equilibrium position that is typically at a lower energy. In doing so, the atoms must transit an energy barrier on the potential energy surface, usually at a saddle point on the surface where the energy barrier is lowest. This process leads to the formation of a defect.

Let $F(t)$ be the probability that a defect has not formed during the process, so that $F(0) = 1$ and $F(t \to \infty) = 0$. The basic equation of TST is

$$\frac{\mathrm{d}F}{\mathrm{d}t} = -k(t)F(t), \tag{1}$$

where $k(t)$ is the rate at which atoms cross the energy barrier. It has the elementary exact solution

$$F = \exp\left(-\int_0^t k(\tau)\,\mathrm{d}\tau\right). \tag{2}$$

The difficulty in applying TST lies in the ability to estimate the rate factor k. A fairly simple expression for this quantity may be obtained by invoking the well-known harmonic approximation (Vineyard 1957, Voter and Doll 1984). This makes use of the fact that the potential energy surface in the neighborhood of an equilibrium position is, to leading order in the atomic positions, a quadratic well. Hence for a system of N atoms with the coordinate axes aligned with the principal curvatures of the potential energy surface,

$$V(\boldsymbol{r}) = V(0) + \frac{1}{2}\left(\kappa_1 r_1^2 + \kappa_2 r_2^2 + \cdots + \kappa_{3N} r_{3N}^2\right). \tag{3}$$

Here the origin is taken to be at the equilibrium position, and the r_i measure the deviation of the atomic positions from equilibrium. The κ_i are simply related to the principal curvatures of the potential energy surface and hence to the eigenvalues of the Hessian matrix for $V(\boldsymbol{r})$. A similar equation can be written at the saddle point $\boldsymbol{r}_s$, where, by definition, one of the principal curvatures of the surface vanishes. Let the corresponding values of the curvature at the saddle point be λ_i and take $\lambda_{3N} = 0$. The

$$V(\boldsymbol{r}) = V(\boldsymbol{r}_s) + \frac{1}{2}\left(\lambda_1 r_1^2 + \lambda_2 r_2^2 + \cdots + \lambda_{3N-1} r_{3N-1}^2\right). \tag{4}$$

We neglect possible temperature effects upon the potential energy surface, a point about which we will have more to say later. A somewhat detailed analysis (Vineyard 1957), which we do not reproduce here, then yields

$$k = \frac{N_s}{2\pi}\sqrt{\frac{1}{m}}\frac{\prod_{i=1}^{3N}\sqrt{\kappa_i}}{\prod_{i=1}^{3N-1}\sqrt{\lambda_i}}\mathrm{e}^{-\Delta E/k_{\mathrm{B}}T} \tag{5}$$

for a system of identical atoms each having mass m. Here ΔE is the energy barrier, $\Delta E = V(\boldsymbol{r}_s) - V(0)$, and N_s is the number of equivalent defect nucleation sites.

In order to compute k from equation (5), we require values for the quantities κ_i and λ_i, as well as for the energy barrier ΔE. These we obtain from a recently developed criterion for zero-temperature defect initiation, called the Wallace criterion. This criterion has been shown to yield accurate predictions of the point (deformation, load, etc) at which defect initiation may be expected in a variety of circumstances (Delph *et al* 2009, Delph and Zimmerman 2010, Yun *et al* 2011). Because it is important to the development of the present model, we give a brief description here. The basic assumption underlying the Wallace criterion is that defect nucleation may be adequately described in terms of the motion of a limited number of atoms surrounding the nucleation site, without the need to take into account the motion of all the atoms in the assemblage. Accordingly, the Wallace criterion envisions a region Ω interior to a much larger atomic assemblage. This region contains N atoms that are allowed to undergo arbitrary infinitesimal motions, with the atoms exterior to Ω being held motionless. The system is stable when all possible motions of the atoms within Ω lead to an increase in system energy. Instability and subsequent defect nucleation is signaled when the change in energy resulting from a particular pattern of atomic motions is found to be negative. Mathematically, stability translates into a requirement that all eigenvalues of the Hessian matrix of the potential energy for the system of N atoms be positive. An instability is indicated when the lowest eigenvalue passes through zero and becomes negative. Typical values of N range from several hundred to in excess of a thousand, depending upon the nature of the loading and the geometric configuration.

At a given equilibrium point, it is simple to show that the eigenvalues obtained from the Hessian matrix are simply half of the κ_i values. A similar statement can be made at the saddle point with regard to the λ_i values, where, by definition, the lowest eigenvalue of the

Hessian matrix vanishes. Detailed expressions for the Hessian matrices for two-body and EAM potentials may be found in Delph *et al* (2009) and Delph and Zimmerman (2010), respectively. It is important to point out in this connection that, regardless of the form of the interatomic potential used, the computation of the Hessian matrix requires a knowledge of the zero temperature atomic positions of the system of N atoms. In simple situations involving homogeneous deformation, this may be obtained, for example, from the Cauchy–Born hypothesis. More complicated situations require detailed numerical computation, such as the use of molecular statics codes. Besides the curvature values, the Wallace criterion likewise yields the energy barrier ΔE as the difference between the potential energy associated with the N atoms at the saddle point and that at the equilibrium point. Expressions for this quantity may be found, for two-body and EAM potentials respectively, in Delph *et al* (2009) and Delph and Zimmerman (2010).

We return to the basic TST equation (2). Under constant-load, equilibrium conditions, the rate factor is time-independent, and equation (2) becomes

$$F = \exp(-kt)\,. \tag{6}$$

However in many circumstances, the crystal is loaded in a time-dependent fashion and in this case, the rate factor varies with time. Let $\varsigma(t)$ be a characteristic parameter that describes the loading process, monotonically increasing with t and with $\zeta(0) = \zeta_o$. Various stress measures have been used in this role, e.g., Mason *et al* (2006), Zhu *et al* (2008), but we prefer to use a more immediately accessible loading parameter, with the choice depending upon the circumstances. In any case, a simple change of variables in equation (2) gives (Mason *et al* 2006)

$$F = \exp\left(-\frac{1}{\dot{\zeta}}\int_{\zeta_o}^{\zeta} k(\xi)\,\mathrm{d}\xi\right), \tag{7}$$

where, as usual, the superposed dot indicates time differentiation. If $k(\zeta)$ is known at points along the loading path, then the integral in equation (7) may easily be evaluated by numerical quadrature to determine $F(\zeta)$.

The overall approach to be adopted here is to move upward along the loading path on the potential energy surface through a succession of equilibrium positions. At each of these positions, the $3N$ eigenvalues of the Hessian matrix are calculated. These yield the κ_i values required in the numerator of equation (5). The energy associated with the reduced ensemble of atoms contained within Ω may be calculated at this position as well. As the point of zero-temperature defect initiation is approached, the lowest eigenvalue decreases. When this value goes through zero, the saddle point has been located. The remaining $3N - 1$ positive eigenvalues at this point give the λ_i's in the denominator of equation (5). Likewise the energy associated with the N atoms within Ω may be calculated to obtain the saddle point energy. The difference between this latter quantity and the energy at a given equilibrium position yields ΔE. From this, the TST rate quantity k may be calculated for any desired number of points along the loading path. Finally, then, F may be calculated by a numerical quadrature procedure from equation (7). The variation of this quantity from 1 down to 0 establishes bounds for the range of the loading parameter over which defect nucleation is predicted to occur.

3. Examples

We reexamine two examples of zero-temperature defect initiation presented in Delph *et al* (2009) and Delph and Zimmerman (2010). The zero-temperature defect behavior has been well established for both of these cases. Our intent here is to show how hTST allows the inclusion of loading rate and temperature effects upon defect initiation.

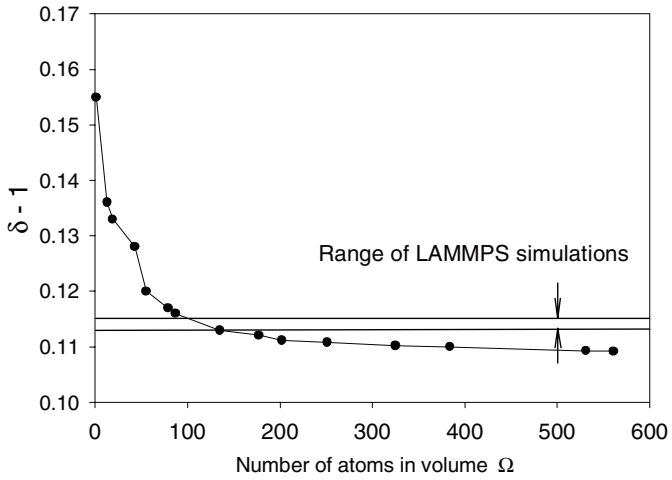

Figure 1. Critical instability stretch for triaxial stretching at $T = 0\,\mathrm{K}$ versus number of atoms contained within Ω.

The first example involves triaxial stretching of a perfect fcc crystal along the principal crystallographic directions. The interatomic potential in this case was taken to be a Lennard-Jones potential, modified to yield smooth second derivatives at the cutoff (van der Eerden *et al* 1992). Let the stretch ratio be $\delta(t)$, and identify the loading parameter ζ with the stretch ratio, so that equation (6) becomes

$$F = \exp\left(-\frac{1}{\dot{\delta}}\int_1^{\delta} k(\xi)\,\mathrm{d}\xi\right). \tag{8}$$

As discussed in Delph *et al* (2009), at a certain critical stretch ratio δ_c, the crystal lattice becomes unstable and a defect in the form of a spherical cavity is nucleated. The atomic array for this example was taken to be an assemblage of $8 \times 8 \times 8$ unit cells containing a total of 2048 atoms subjected to periodic boundary conditions along each face. The region Ω was a sphere centered within the assemblage.

The Wallace criterion, and hence the hTST model presented in the previous section, is, to a certain point, sensitive to the number of atoms N contained within this region. Figure 1 shows the zero temperature critical stretch ratio at which cavitation will occur as computed from the Wallace criterion for various values of N. It can be seen that for values of N in excess of about 300, the value of δ_c is essentially constant, and is, moreover, in good agreement with independent simulations carried out with the LAMMPS MD code[5] (LAMMPS 2012), the results from which are also shown in the figure. It will be noted, moreover, that a value of $N = 1$ yields a value of δ_c that is approximately 50% in error. Arguing from the zero-temperature results shown in figure 1, values of N on the order of 300–500 can be expected to yield accurate results in the hTST model.

Figure 2 shows the hTST results for two different constant stretch rates, $\dot{\delta} = 10^6\,\mathrm{s}^{-1}$ and $\dot{\delta} = 10^{10}\,\mathrm{s}^{-1}$ and for two different values of N, $N = 321$ and $N = 555$, at a temperature of 20 K ($T_{\mathrm{melt}} = 72\,\mathrm{K}$ for this material). Because cavitation is equally likely to occur anywhere

[5] These LAMMPS simulations involved various-sized systems (4000 to 32000 atoms) subjected to quasi-static, equitriaxial stretches. Each system was equilibrated at a fixed amount of stretch using a conjugate gradient energy minimization algorithm, with stretch being incrementally increased until cavitation occurred. Like the system analyzed using the Wallace method, the LAMMPS systems were subjected to periodic boundary conditions in all directions.

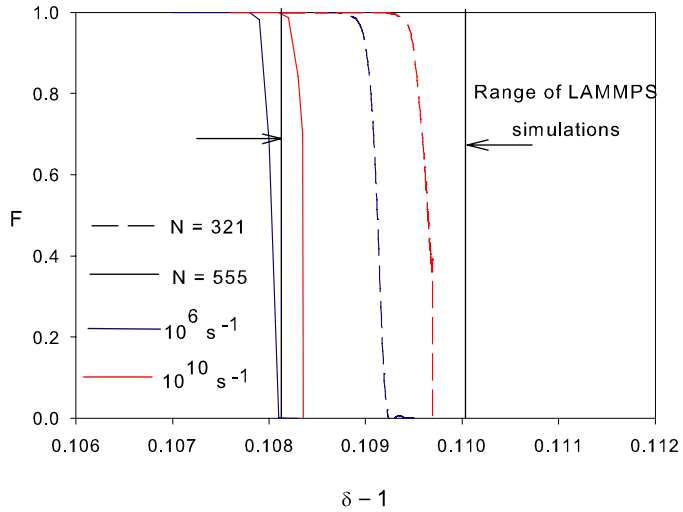

Figure 2. hTST predictions for triaxial stretching for stretch rates of 10^6 and $10^{10}\,s^{-1}$.

Table 1. Calculated values of prefactor and energy barrier for the triaxial stretching of an fcc crystal using the Wallace + hTST method for two different values of N.

	$N = 321$		$N = 555$	
$\delta - 1$	Prefactor (s^{-1})	Energy Barrier (eV)	Prefactor (s^{-1})	Energy barrier (eV)
0.105	4.091×10^{52}	0.320	1.357×10^{62}	0.396
0.106	1.568×10^{44}	0.251	2.725×10^{47}	0.278
0.107	3.265×10^{35}	0.183	1.581×10^{32}	0.160
0.108	3.396×10^{26}	0.115	1.551×10^{16}	0.042
0.109	1.411×10^{17}	0.047		Instability

within the atomic array, N_s was taken to be 2048. The corresponding values for the prefactor (defined as the coefficient of the exponential term in equation (5) less the N_s term) and the energy barrier are given in table 1 for both values of N.

First of all, it can be seen that F varies rapidly from 1 to 0 over a narrow range of stretches, yielding tight predictions for the range of stretch ratios over which cavitation may be expected. The effect of the stretching rate upon the cavitation behavior is evident. Independent MD simulations were conducted for this situation over the stretch rate range 10^6–$10^{10}\,s^{-1}$ using the LAMMPS code, and the bars on the figure show the range of predicted cavitation stretches. These simulations used a slightly larger system of $10 \times 10 \times 10$ unit cells (4000 atoms) that is first equilibrated at 20 K and zero pressure for a period of 100 ps (10^5 time-steps of 0.001 ps/step) using a Nosé–Hoover combination thermostat/barostat (NPT) algorithm for the isothermal–isobaric ensemble. The system is then expanded triaxially at a uniform engineering stretch rate with a time-integrator corresponding to a microcanonical (NVE) ensemble, a practice commonly done in molecular simulations. Further details about these algorithms can be found on the LAMMPS website: http://lammps.sandia.gov.

In general, the LAMMPS results show somewhat more stretch rate sensitivity than does the hTST model, but the overall agreement between the two is quite good. We note, however, that the validity of the hTST model at the highest stretch rate is questionable, a point upon which we expand in the appendix.

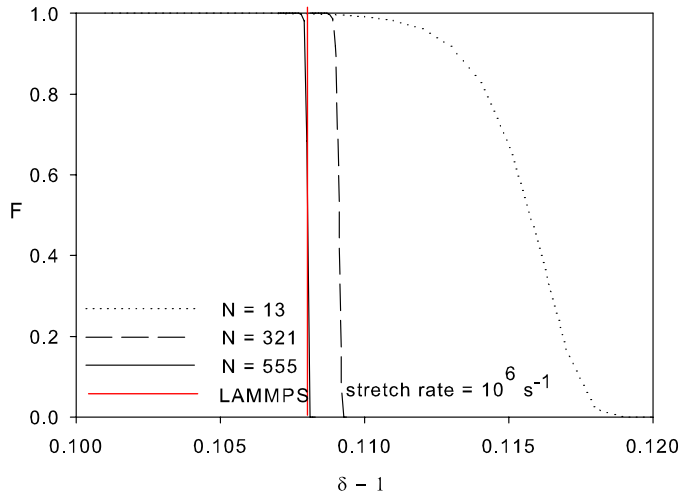

Figure 3. Variation of predicted defect nucleation stretch with N.

Figure 3 shows the effect of increasing the value of N upon the results. As we noted earlier in connection with zero-temperature instabilities, the use of too small a value of N leads to inaccurate predictions. However, for values of N sufficiently large so that the zero-temperature instability stretch becomes insensitive to further increases in this quantity, predictions of defect nucleation likewise become insensitive to increases in N. As figure 3 demonstrates, small values of N, e.g., $N = 13$, considerably over-predict the stretch at which nucleation may be expected. However larger values of N lying on the flattened portion of figure 1 give consistent predictions that are in good agreement with MD simulations.

We now pass to a considerably more complicated example, that of nanoindentation of a gold crystal on its (0 0 1) surface. Here the interatomic potential was taken to be an EAM-type potential (Voter 1993), and the region Ω a rectangular solid whose upper surface was coincident with the free surface of the Au crystal and centered upon the indenter. The atomic positions required to compute the Hessian matrix were taken directly from zero-temperature LAMMPS simulations, carried out at successive increments of 0.01 Å of indenter depth. The loading parameter ζ in this case was taken to be the indentation depth d. For sufficiently large indentation depths d, a V-shaped dislocation structure was nucleated at four to five atomic planes beneath the indenter. The zero-temperature nucleation behavior in this case is discussed in more detail by Delph and Zimmerman (2010). However of particular interest is the fact that, for small indentation depths, the defect was found to be reversible, that is, it disappeared if the indenter were raised. We discuss this point at greater length in the discussion.

Computations were carried out for two different indentation rates, $\dot{d} = 10^9$ Å s^{-1} and $\dot{d} = 10^{11}$ Å s^{-1}, and for two different values of $N = 486$ and $N = 845$, values that were found to yield accurate results for the zero-temperature dislocation nucleation behavior (Delph and Zimmerman 2010). It was assumed that dislocation nucleation could occur in any one of a $3 \times 3 \times 3$ block of unit cells underneath the indenter, leading to a value of $N_s = 108$. Values for the prefactor and the energy barrier are given in table 2 for both values of N. Figures 4 and 5 show, respectively, the results obtained from the hTST model at two different temperatures, $T = 100$ K and $T = 300$ K.

The range of indentation depths over which dislocation nucleation occurs in independent LAMMPS simulations is indicated on both figures. These simulations are performed on a system approximately 50 × 50 × 30 unit cells (30 0000 atoms) for which the bottom

Table 2. Calculated values of prefactor and energy barrier for the indentation of an fcc crystal by a 40 Å radius spherical indenter using the Wallace + hTST method for two different values of N.

	$N = 486$		$N = 845$	
d (Å)	Prefactor (s^{-1})	Energy barrier (eV)	Prefactor (s^{-1})	Energy barrier (eV)
2.83	8.137×10^{10}	0.396	2.930×10^{10}	0.378
2.84	7.186×10^{10}	0.340	2.478×10^{10}	0.281
2.85	3.969×10^{10}	0.284	6.304×10^{9}	0.183
2.86	3.770×10^{10}	0.222	4.586×10^{9}	0.077
2.87	1.813×10^{10}	0.167		Instability
2.88	1.735×10^{10}	0.107		
2.89	1.478×10^{10}	0.048		

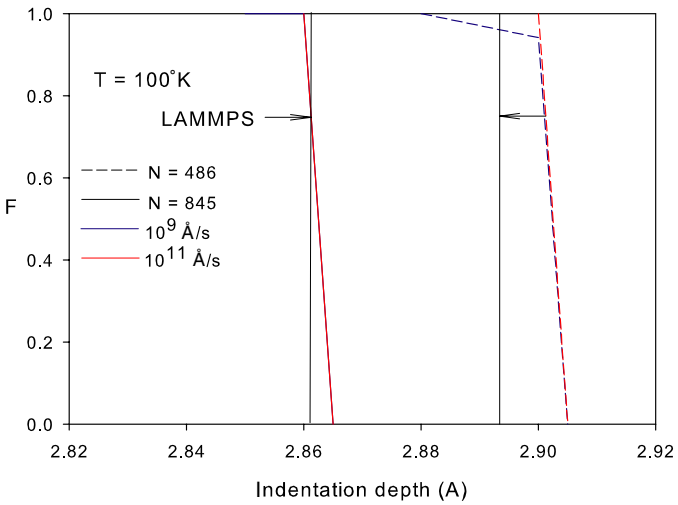

Figure 4. hTST predictions for nanoindentation at $T = 100$ K.

20 000 atoms are held fixed and the remaining atoms are equilibrated to temperature (100 or 300 K) within 30 ps (30 000 time-steps of 0.001 ps/step). Indentation was done by prescribing a quadratic force-field from the center of a rigid sphere of radius 40 Å that moves downward, penetrating the top layer of the system at one of the rates given above. Details about the algorithm for performing dynamic indentation can be found on the LAMMPS website: http://lammps.sandia.gov.

Regarding both figures 4 and 5, we take note of the fact that the F versus d curves are, on the scale of the horizontal axis, computed rather coarsely because the zero-temperature LAMMPS results from which the Hessian matrix was computed were available only at intervals of 0.01 Å. Nevertheless, the overall trends are clear. As was the case with the stretching example considered previously, the hTST predictions yield tight bounds for the range of indentation depths over which dislocation nucleation is to be expected. These are in very good accord with the LAMMPS results. Once again, however, the LAMMPS results demonstrate somewhat greater rate sensitivity than is the case with those obtained from the hTST model, especially at the higher value of N.

A major advantage of the TST approach to defect nucleation is that it is not limited to the high rates typical of MD simulations. Figure 6 illustrates this feature, showing hTST predictions ranging from $\dot{d} = 10^{11}$ Å s^{-1} down to $\dot{d} = 100$ Å s^{-1}, a factor of 10^9 variation in

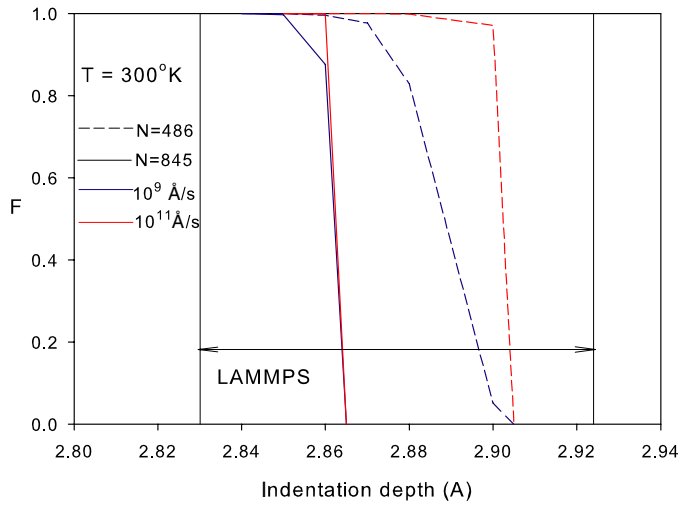

Figure 5. TST predictions for nanoindentation at $T = 300$ K.

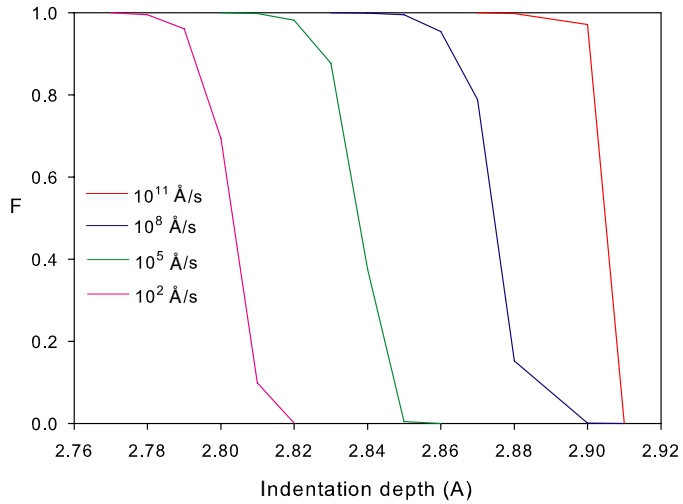

Figure 6. TST predictions for nanoindentation at $T = 300$ K with $N = 486$, with indentation rates varying from MD-scale down to laboratory scale.

indentation rates. The lowest of these values is typical of those achievable in the laboratory. The rate sensitivity of the dislocation nucleation process is evident.

Finally, we consider the situation in which the indentation depth is held at a constant value. It has been observed experimentally in these cases that, after some period of time, dislocation nucleation may occur spontaneously underneath the indenter (Ngan *et al* 2006). Here F may be computed very simply from equation (6), given the rate factor k at a given indentation depth d. Figure 7 shows the variation of the time required to reach a value of $F = 0.5$ for various values of indentation depth at $T = 300$ K and for $N = 486$, which is roughly a measure of the average time required for dislocation nucleation. It can be seen that a variation in indentation depth of just 0.1 Å produces a variation in average dislocation nucleation time of over 10 orders of magnitude.

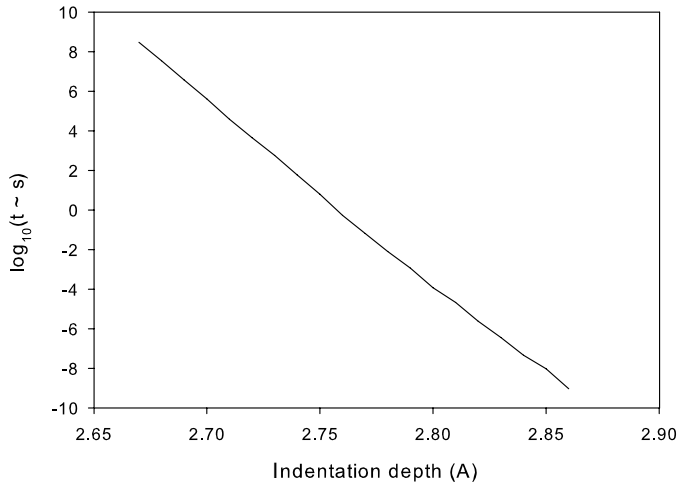

Figure 7. Time required to reach a value of $F = 0.5$ under constant indentation depth.

4. Discussion

We have presented here a harmonic transition state (hTST) theory model for defect initiation in crystals that differs in several significant respects from earlier work, most notably in the manner in which the prefactor and the energy barrier in equation (5) are calculated. It draws upon a recently developed model for zero-temperature defect initiation known as the Wallace criterion (Delph *et al* 2009, Delph and Zimmerman 2010, Yun *et al* 2011). The Wallace criterion has shown itself to be quite accurate in making predictions of defect nucleation in the low-temperature regime for which temperature and rate effects are absent. The ability to do this at zero temperature is, of course, a very desirable feature in a model that seeks to predict temperature and temperature-associated effects. The Wallace criterion has several other marked advantages with regard to hTST.

One is that it produces directly the potential energy surface curvatures for the hTST rate factor in equation (5). Several previous TST models have made use of one-dimensional models in which the hTST rate factor contains a single constant curvature component. Equation (5), on the other hand, makes use of a considerably more accurate expression in which the prefactor involves a fairly large number of curvature components. These curvature components, in addition, vary from point to point along the loading path. At least with regard to the indentation example presented, the use of just a single constant curvature component can underestimate the prefactor in equation (5) by as much as 70%, as compared to the more accurate model presented here. However in practice, the hTST rate factor was found to be relatively insensitive to the value of the prefactor, as the rate factor was dominated by the exponential energy barrier term.

Here the Wallace criterion yields the energy barrier to defect nucleation in a direct fashion as the difference between the saddle point energy associated with the group of N atoms and that at a given point along the loading path. The saddle point is located in straightforward fashion by moving sequentially upward along the loading path on the potential energy surface until reaching the point at which the lowest eigenvalue of the Hessian matrix vanishes. This is coincident with the zero-temperature instability point (Delph *et al* 2009, Delph and Zimmerman 2010, Yun *et al* 2011). This procedure, of course, implicitly assumes that the loading path is the transition path along which defect nucleation proceeds. Previous work in this area has

made use of variations on the nudged elastic band (NEB) technique to determine the energy barrier. The goal of the NEB technique is to determine the so-called minimum energy path between an initial undefected state and a final defected shape, which is the transition path of greatest statistical significance. The technique employed here to determine the energy barrier is hence of a somewhat *ad hoc* nature, since the path between the current state and the saddle point state is not necessarily the minimum energy path between current and defected state, and therefore may overestimate to some extent the actual size of the energy barrier. We justify this method by the fact that the results are in good agreement with the results of MD simulations for two very different situations. Moreover, the values of the energy barriers obtained by this method (tables 1 and 2) are in very reasonable agreement with NEB-obtained values reported by other investigators, e.g., Nguyen *et al* (2011).

In any case, the NEB method is of questionable applicability to the example problems considered in the manuscript. The reason for this is that the NEB method, at least as it is currently implemented, requires that the external load or deformation be the same for both the initial undefected and the final defected states. Physically, this is a result of the implicit assumption that the thermal processes leading to defect nucleation are much faster than the loading/deformation process, a point which we address in the appendix in another context. This requirement is predicated on the condition that the final defected state be stable under the same loading/deformation condition. Alternatively, this condition can be expressed as one of irreversibility, i.e. the defect must persist when the system is brought to the load/deformation level for the initial state. Our analysis of the nanoindentation example indicates that this requirement is not satisfied by the initially formed defect, which was found to disappear as the indenter was raised incrementally to return to its position at the initial state. Such reversible defect behavior is not uncommon in atomistic simulations, e.g. Zimmerman *et al* (2009). Our example problem of cavitation is also difficult to treat with the NEB method, as the final, equilibrated state is quite 'far' in the potential energy landscape from the point at which the instability begins.

Moreover, the NEB method requires an *a priori* assumption as to the nature of the nucleated defect in order to define the end state for the NEB calculation. The value of the energy barrier thus computed may be expected to be sensitive, to a greater or lesser extent, to the accuracy of this assumption. The method used here, by contrast, requires no such advance knowledge.

As was found to be the case at zero temperature (Delph *et al* 2009, Delph and Zimmerman 2010, Yun *et al* 2011), moderately large values of N are required to obtain accurate results with the present model. Physically, this is a reflection of the fact that defect initiation involves the coordinated motion of a fairly large number of atoms (Miller and Rodney 2008). We have not attempted here to carry out formal convergence studies of the predictions of our model as a function of N. However, we feel that the results shown here demonstrate reasonable convergence, given the trends shown in figure 3 and the fact that a near doubling of the value of N in figures 4 and 5 shifts the curves by only about 0.04 Å.

We have neglected the effects of temperature upon the potential energy surface itself. We feel that this represents a reasonable approximation at moderate temperatures, as the results presented here demonstrate. At higher temperatures, however, such effects may well be important, and have been a source of concern in the recent literature, e.g. Zhu *et al* (2008), Warner and Curtin (2009), Hara and Li (2010), Ryu *et al* (2011). In order to account at least to some extent for these temperature effects, Ryu *et al* (2011) have introduced a formulation in which the TST energy barrier is given in terms of a free energy barrier, and which contains, by consequence, an entropic term. We note that the present TST model may also be posed in this fashion if one adopts the harmonic approximation for the entropy (Vineyard 1957). In

particular, if we write equation (5) as

$$k = \nu^* \mathrm{e}^{-\Delta E/kT}, \tag{9}$$

then Vineyard (1957) showed that one may also write

$$k = \tilde{\nu} \mathrm{e}^{-\Delta F/kT}, \tag{10}$$

where ΔF is the Helmholtz free energy barrier, with

$$\nu^* = \tilde{\nu} \mathrm{e}^{\Delta S/k}. \tag{11}$$

Using the harmonic approximation for the entropy, one may represent the entropic factor in equation (11) entirely in terms of quantities defined upon the potential energy surface. This yields a formulation identical to that presented here. See also Weiner (2002) in this connection. Thus, although they do not appear explicitly, the model presented here considers entropic effects within the context of the harmonic approximation (sometimes also known as the vibrational contribution to the entropy). One may, however, question the accuracy of the harmonic approximation to the entropy, as Ryu *et al* (2011) have done. These authors have pointed to configurational effects such as increases in the lattice constant with increasing temperature that will act to affect the potential energy surface. Moreover the lattice itself will become increasingly disordered as the melting temperature is approached. On the other hand, the very good agreement between the hTST model predictions and MD simulations for the examples presented here seems to indicate that such contributions to the entropy are not particularly significant for these cases.

In terms of the physics of the defect initiation process, the present results indicate that defect nucleation is very sensitive to the loading parameter. For example, for the nanoindentation example presented here, defect initiation occurs over a range of indenter depths on the order of just several hundredths of an angstrom. Moreover under static loading, a variation in indenter depth of as little as 0.1 Å results in a variation in mean indentation time of over 10 orders of magnitude.

Previous work with TST models have involved scenarios in which the initial, pre-defected state was one of uniform deformation, either uniaxial tension, compression, or simple shear. The nanoindentation example treated here is, by contrast, much more complicated than earlier efforts along these lines. This was accomplished in part by the use of large-scale molecular statics codes to determine the zero-temperature interatomic spacings, a technique that is generally valid for complex inhomogeneous deformation states. This, of course, requires a not-inconsiderable numerical effort. This effort may be mitigated to some extent by the use of hybrid continuum-atomistic techniques, such as the quasi-continuum method, e.g. Miller and Tadmor (2002), for especially large systems, but may still be substantial. Such an effort would not be justified were it not for the fact that TST models have the ability to reach much slower loading rates and much longer time scales than are accessible to molecular dynamics codes.

At the opposite end of the scale, it is worth pointing out that TST models are of questionable validity at very high loading rates or on very short time scales, including some of the highest rates presented here. Because comparisons between MD simulations and TST models have been frequent in the literature, we discuss this issue in somewhat more detail in the appendix.

Based upon the very good agreement with independent molecular dynamics simulations, we believe the hTST model described here to be capable of making reliable predictions of temperature and rate effects upon defect nucleation. For reasons that are yet unclear, the hTST results show somewhat less rate dependence than do the numerical simulations. This may indicate a deficiency in the hTST approximation. However, the overall agreement is still very satisfactory. Accordingly we feel that this model represents a promising tool for defect prediction at non-zero temperatures and at laboratory loading rates and time scales.

Acknowledgments

The authors are grateful to Professor Ting Zhu and Dr Aidan Thompson for helpful conversations. PC acknowledges a Dean's Fellowship from Boston University and HSP acknowledges NSF grant CMMI-1036460 in support of this research. Sandia National Laboratories is a multi-program laboratory managed and operated by Sandia Corporation, a wholly owned subsidiary of Lockheed Martin Corporation, for the US Department of Energy's National Nuclear Security Administration under contract DE-AC04-94AL85000.

Appendix

We address here the question of the upper limit of validity of TST models at high loading rates or short time scales by means of a simple, order-of-magnitude argument. The basic picture underlying TST is that a group of atoms oscillating in a potential energy well. Randomly, and after a sufficient number of oscillations, the atoms acquire sufficient kinetic energy to make the jump into an adjacent potential energy well. One means by which loading or deformation rate could affect this picture would be if the deformation rate were to change the nature of the atomic configuration, and hence the underlying potential energy surface, on a considerably shorter time scale than would be required for the atoms to leave that configuration and transition to another. Put slightly differently, TST assumes that the potential energy surface is static, but if this were not the case and if the potential energy surface were changing on a time scale faster than the period of atomic oscillation, then the validity of TST would be questionable. An estimate of the limits of validity of TST under high deformation rate may then be obtained by comparing the time required to 'significantly' change the atomic configuration to that of the period of atomic oscillation.

We focus on the uniform stretching example set forth previously for which the stretch rates ranged from $\dot{\delta} = 10^6 - 10^{10}\,\mathrm{s}^{-1}$. Similar, although necessarily more complicated, estimates can be made for the nanoindentation example, although we do not attempt them here. In any case, the increment in stretch over a given time increment Δt is simply $\Delta\delta = \dot{\delta}\Delta t$. Assume as a reasonable estimate that a 1% increase in stretch is the greatest stretch that could be sustained without 'appreciably' changing the nature of the potential energy surface. Then at the highest stretch rate of $\dot{\delta} = 10^{10}\,\mathrm{s}^{-1}$,

$$\Delta t_{\min} \sim \frac{0.01}{10^{10}} = 10^{-12}\,\mathrm{s}. \tag{A1}$$

Now we need to calculate the period of atomic oscillation. The minimum positive eigenvalue extracted from the Hessian matrix at the point of hTST defect nucleation is approximately $k_{\min} = 0.2$ in nondimensional units, or in dimensional units (van der Eerden *et al* (1992)), $k_{\min} = 3.0 \times 10^{-3}\,\mathrm{J\,m}^{-2}$. The potential energy well corresponding to this eigenvalue is $U = \frac{1}{2}k_{\min}x^2$. Given the mass of the argon atom as 6.635×10^{-26} kg, the minimum period of atomic oscillation is therefore

$$T_{\min} = 2\pi\sqrt{\frac{m}{k_{\min}}} = 3.0\ \mathrm{x}\ 10^{-11}\,\mathrm{s}. \tag{A2}$$

Thus, we conclude that a stretch rate of $10^{10}\,\mathrm{s}^{-1}$ strains the limits of validity of TST. For rates that are $10^9\,\mathrm{s}^{-1}$ and lower, the condition $\Delta t_{\min} < T_{\min}$ is satisfied and TST should be valid.

Support for this conclusion can be gained by a careful examination of accompanying MD simulations for this situation. Figure A1 shows the variation of hydrostatic stress with increasing stretch for the triaxial stretching example, while figure A2 shows the variation of temperature. The simulations performed here used a system of 4000 atoms initially at a

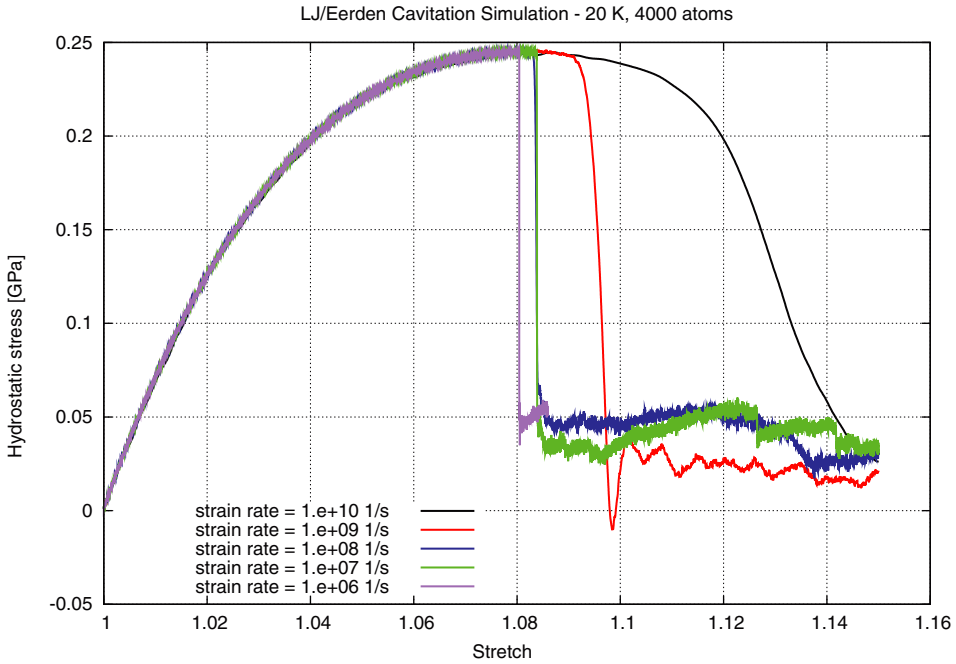

Figure A1. Variation of hydrostatic stress with stretch for stretch rates varying from 10^6 to 10^{10} s^{-1}.

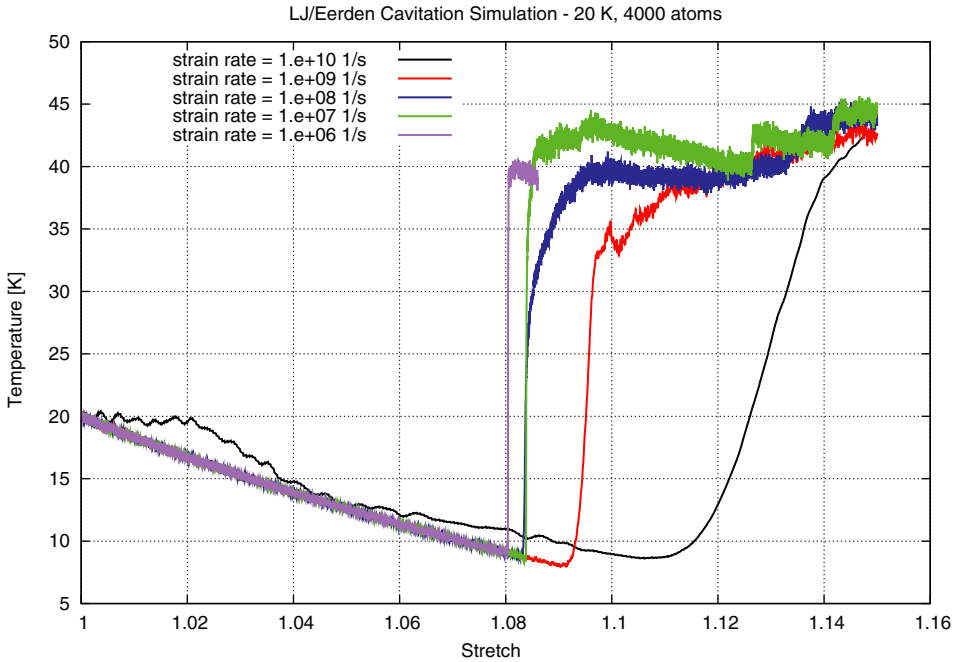

Figure A2. Variation of temperature with stretch for stretch rates varying from 10^6 to 10^{10} s^{-1}.

temperature of $T = 20\,\mathrm{K}$. The simulation is not run isothermally; rather, the equations of motion for a microcanonical (NVE) ensemble are used in conjunction with the application of a uniform stretch rate that expands the system over time. As a result and as shown in figure A2, the system experiences adiabatic cooling in the elastic regime followed by rapid heating during the initiation of defects and onset of plastic deformation. This same behavior was noticed by Seppälä *et al* (2004). Simulations were also performed for significantly larger systems (108 000 atoms), which produced similar graphs with the same trends as shown in figures A1 and A2.

Figures A1 and A2 clearly show that for stretch rates from $10^9\,\mathrm{s}^{-1}$ down to $10^6\,\mathrm{s}^{-1}$, the system follows essentially the same trajectory in the evolution of temperature and stress with increasing stretch, at least up to the instability point of defect initiation. We do notice some dependence of the stretch associated with this instability point on the loading rate, but this difference is minor for the three lowest rates and appears to be converging as rate decreases. In contrast to rates $\leqslant 10^9\,\mathrm{s}^{-1}$, we observe that the system follows a decidedly different path at a stretch rate of $10^{10}\,\mathrm{s}^{-1}$, even in the elastic regime, with the instability point much less clearly defined. These stress and temperature curves support the hypothesis that at the highest rate ($10^{10}\,\mathrm{s}^{-1}$) the potential energy surface is changing as fast as the atomic oscillations allow exploration of that surface, whereas at lower rates ($10^9\,\mathrm{s}^{-1}$ and below) the surface is static relative to the speed of this exploration.

References

Delph T J and Zimmerman J A 2010 *Modelling Simul. Mater. Sci. Eng.* **18** 045008
Delph T J, Zimmerman J A, Rickman J M and Kunz J M 2009 *J. Mech. Phys. Solids* **57** 67
Hara S and Li J 2010 *Phys. Rev.* B **84** 184114
Henkelman G, Uberuaga B and Jónsson H. 2000 *J. Chem. Phys.* **113** 9901
Henriksen N E and Hansen FY 2008 *Theories of Molecular Reaction Dynamics* (Oxford: Oxford University Press)
Jin C, Ren W and Xiang Y 2010 *Scr. Mater.* **62** 206
LAMMPS 2012 http://lammps.sandia.gov
Mason J K, Lund A C and Schuh C A 2006 *Phys. Rev.* B **73** 054102
Miller R E and Rodney E 2008 *J. Mech. Phys. Solids* **56** 1203
Miller R E and Tadmor E B 2002 *J. Comput.-Aided Mater. Des.* **9** 203
Ngan A H W, Zuo L and Wo P C 2006 *Proc. R. Soc.* A **462** 1661
Nguyen L D, Baker K L and Warner D H 2011 *Phys. Rev.* B **84** 024118
Ryu S K, Kang K and Cai W 2011 *Proc. Natl Acad. Sci.* **108** 5174
Seppälä E T, Belak J and Rudd R E 2004 *Phys. Rev.* B **69** 134101
van der Eerden J P, Knops H J F and Roos A 1992 *J. Chem. Phys.* **96** 714
Vineyard G H 1957 *J. Phys. Chem. Solids* **3** 121
Voter A F 1993 *Technical Report* LA-UR 93-3901 Los Alamos National Laboratory
Voter A F and Doll J D 1984 *J. Chem. Phys.* **80** 5832
Warner D H and Curtin W A 2009 *Acta Mater.* **57** 4267
Weinberger C R, Jennings A T, Kang K and Greer J R 2012 *J. Mech. Phys. Solids* **60** 84
Weiner J H 2002 *Statistical Mechanics of Elasticity* (New York: Dover)
Yun G, Cao P, Zimmerman J A, Delph T J and Park H S 2011 *Int. J. Solids Struct.* **48** 3406
Zhu T, Li J, Samanta A, Kim H G and Suresh S 2007 *Proc. Natl Acad. Sci.* **104** 3031
Zhu T, Li J, Samanta A, Leach A and Gall K 2008 *Phys. Rev. Lett.* **100** 025502
Zimmerman J A, Bammann D J and Gao H 2009 *Int. J. Solids Struct.* **46** 238